Optical Engineering

OpticalEngineering.SPIEDigitalLibrary.org

Remotely detected vehicle mass from engine torque-induced frame twisting

Troy R. McKay
Carl Salvaggio
Jason W. Faulring
Glenn D. Sweeney

SPIE.

Troy R. McKay, Carl Salvaggio, Jason W. Faulring, Glenn D. Sweeney, "Remotely detected vehicle mass from engine torque-induced frame twisting," *Opt. Eng.* **56**(6), 063101 (2017), doi: 10.1117/1.OE.56.6.063101.

Remotely detected vehicle mass from engine torque-induced frame twisting

Troy R. McKay,* Carl Salvaggio, Jason W. Faulring, and Glenn D. Sweeney
Rochester Institute of Technology, Chester F. Carlson Center for Imaging Science, College of Science, Digital Imaging and Remote Sensing Laboratory, Rochester, New York, United States

Abstract. Determining the mass of a vehicle from ground-based passive sensor data is important for many traffic safety requirements. This work presents a method for calculating the mass of a vehicle using ground-based video and acoustic measurements. By assuming that no energy is lost in the conversion, the mass of a vehicle can be calculated from the rotational energy generated by the vehicle's engine and the linear acceleration of the vehicle over a period of time. The amount of rotational energy being output by the vehicle's engine can be calculated from its torque and angular velocity. This model relates remotely observed, engine torque-induced frame twist to engine torque output using the vehicle's suspension parameters and engine geometry. The angular velocity of the engine is extracted from the acoustic emission of the engine, and the linear acceleration of the vehicle is calculated by remotely observing the position of the vehicle over time. This method combines these three dynamic signals; engine induced-frame twist, engine angular velocity, and the vehicle's linear acceleration, and three vehicle specific scalar parameters, into an expression that describes the mass of the vehicle. This method was tested on a semitrailer truck, and the results demonstrate a correlation of 97.7% between calculated and true vehicle mass. [DOI: 10.1117/1.OE.56.6.063101]

Keywords: video tracking; vehicle mass; engine torque; frame twist.

Paper 161619 received Oct. 17, 2016; accepted for publication May 23, 2017; published online Jun. 8, 2017.

1 Introduction

Overloaded commercial vehicles increase the risk of accidents and cause deterioration of roads and bridges. It is estimated that 6% of the total truck population is illegally overloaded.[1] When trucks are loaded in excess of their maximum permitted limit, they become less stable due to an elevated center of gravity which can over-strain the on-board stability systems, increasing the potential for rollover accidents and jack-knifing.[2] The braking capacity of a truck can be significantly reduced due to overloading.[2] Other risks associated with the operation of heavily laden vehicles include an increased chance of a tire blowout and a higher likelihood of fire.[2] Overloaded vehicles also cause accelerated wear to roads and bridges. While passenger vehicles make up the majority of traffic on highways, trucks and other heavy vehicles cause significantly more pavement deterioration, and overloaded trucks and heavy vehicles cause a disproportionate amount of damage.[3] For example, based on the research by Berthelot,[4] a vehicle overloaded by 20% would cause more than double the damage to roadways than the same vehicle loaded at the legal weight limit. Bridges can experience accelerated fatigue damage due to continued exposure to loads exceeding their design limit.[2]

Traditionally, overloading enforcement is carried out by the random weighing of trucks at static weigh stations.[5] The trucks are driven onto scales, and drivers of overloaded trucks are subjected to substantial fines. This method requires the presence of a manned staff of weigh station employees and it takes significant time to weigh the truck and issue the citation to the driver.[2] As a result, not all trucks are weighed, which leads to more drivers pushing the limits and driving overloaded. A method of measuring the mass of a vehicle using a ground-based, real-time, imaging, and acoustic sensor system would increase efficiency and allow overloaded vehicles to be identified and singled out. This would reduce the costs associated with manning a weigh station, allow appropriately loaded vehicles to avoid unwarranted delays, prevent accelerated damage to roadways and bridges, and protect the public from the dangers presented by these overloaded vehicles. This paper discusses the work performed to develop a method for calculating the mass of a vehicle, remotely, using ground-based imaging and acoustic sensors.

2 Background

The method described here exploits Newton's third law to calculate the total mass of a vehicle from measurements of its linear velocity and the rotational energy output by its engine. Consider a typical rear-wheel drive vehicle at rest with its engine idling. To move forward, the rotational energy generated by the engine is transferred to the transmission via the release of the clutch, where the transmission increases the rotational torque and reduces the rotational velocity. The output of the transmission turns the drive shaft, which in turn rotates the rear axle's pinion gear, which turns the rear wheels and propels the vehicle. The total transfer efficiency of this conversion from rotational power to linear power at low linear velocities is determined predominately by the transfer efficiency of the transmission.[6] A typical transmission has an efficiency in the range of 0.85 to 0.95 and varies based on gear.[6]

Per Newton's third law, which states that for every action there is an equal and opposite reaction, the action of the

*Address all correspondence to: Troy McKay, E-mail: troy@hyperspectralsolutions.com

0091-3286/2017/$25.00

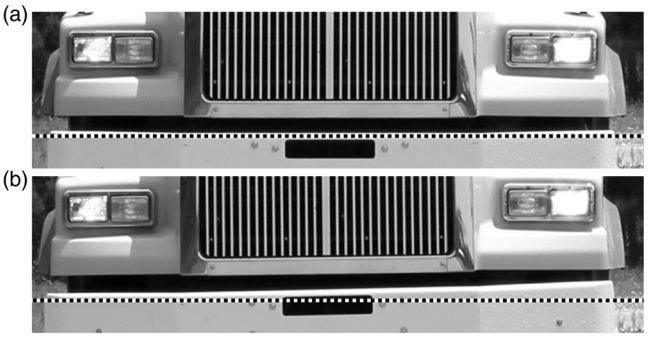

Fig. 1 (a) The vehicle at rest with no engine-induced torque and (b) the vehicle with engine torque-induced frame twist as the vehicle begins to accelerate from a resting state.

applied torque results in an equal and opposite reaction torque. This reaction torque is opposed by the vehicle's suspension as the vehicle's frame rotates relative to its axles. For an engine mounted parallel to the drive shaft, known as a longitudinal engine, this frame twist would manifest as a counter-clockwise rotation (viewing the vehicle head on). The magnitude of this rotation is small, typically less than 2 deg during heavy acceleration. An example of this engine torque-induced frame twisting can be seen in Fig. 1.

Measurements of the engine torque-induced frame twist combined with acoustic measurements of the engine's speed can be used to calculate the energy generated by the engine over a period of time. Given a dry, flat, roadway, and assuming all of the rotation energy generated by the engine is converted into the vehicle's linear kinetic energy, the mass of the vehicle can be determined through measurements of the vehicle's change in velocity. Equation (1) shows the relationship between kinetic energy and mass for linear motion; where KE is the linear kinetic energy of the vehicle, m is the total mass of the vehicle, and x' is the linear velocity of the vehicle. By measuring the rotational power output by the vehicle's engine over a period of time and measuring the change in linear velocity of the vehicle over the same period of time, the mass of the vehicle can be calculated

$$\mathrm{KE} = \frac{1}{2} m \cdot (x')^2. \tag{1}$$

When the engine is applying torque to the vehicle frame τ_E, the frame twists relative to the axles and the vehicle's suspension springs are compressed and stretched as shown in Fig. 2. This compression and stretching of the suspension springs cause pushing and pulling forces to be applied at the points where the frame and suspension are joined. The amount of torque generated by these forces τ_F is dependent on their distance from the axis of rotation r and the amount of frame twist θ as described by Eq. (2) (the cosine term accounts for the force applied nonperpendicularly to the radial axis).[7] The forces F_1 and F_2 are generated by the vehicle's suspension and can be described in terms of the frame twist and the total suspension spring constant k_s as given in Eqs. (3) and (4). By combining these equations, the torque generated by the suspension can be described as a function of frame twist [Eq. (5)]. Since the torque the engine is applying to the frame is equal in magnitude and opposite in direction to the torque the suspension is applying on the

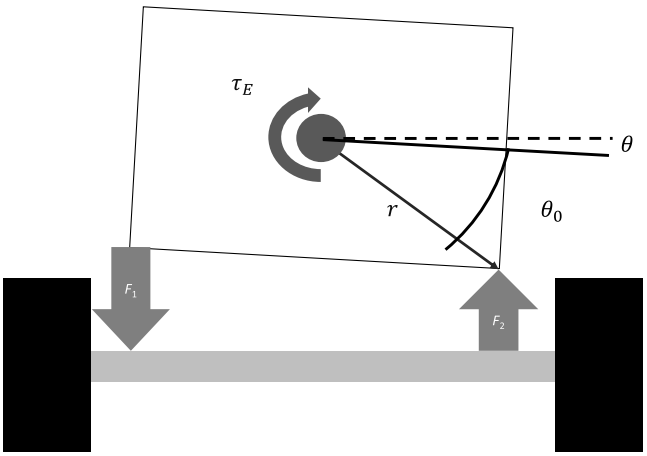

Fig. 2 Longitudinal engine imparting torque τ_E to the vehicle frame causing it to twist until the torque generated by the suspension forces (F_1 and F_2) are sufficient to match.

frame, the engine torque can be described as a function of the frame twist using the relationship described in Eq. (6)

$$\tau_F(t) = r \cdot \cos[\theta(t) + \theta_0] \cdot (F_2 - F_1), \tag{2}$$

$$F_1(t) = -\frac{k_s \cdot r \cdot \tan[\theta(t)]}{2}, \tag{3}$$

$$F_2(t) = \frac{k_s \cdot r \cdot \tan[\theta(t)]}{2}, \tag{4}$$

$$\tau_F(t) = k_s \cdot r^2 \cdot \cos[\theta(t) + \theta_0] \cdot \tan\,\theta(t), \tag{5}$$

$$\tau_E(t) = -k_s \cdot r^2 \cdot \cos[\theta(t) + \theta_0] \cdot \tan\,\theta(t). \tag{6}$$

The expected amount of engine torque-induced frame twist was calculated for an unloaded, half-loaded, and fully loaded semitrailer truck accelerating at a constant rate and can be seen in Table 1. For this calculation, the total suspension spring constant k_s was estimated for a typical semitrailer truck having four leaf springs (two in the front and two in the rear). The engine and suspension geometry parameters (r and θ_0) were estimated for a typical semitrailer truck. This estimation is predicated on the assumption of a flat road and good driving conditions. This frame-twist angle estimation does not take into consideration the efficiency of the transmission, and as a result, will be slightly overestimated. These estimated results show the expected engine torque-induced frame twist values to range from 0.75 deg, for an unloaded semitrailer truck, to 2.15 deg for a fully loaded semitrailer truck. These estimates predict that the frame twist signature should be large enough to measure remotely.

Now that the torque being created by the engine has been described in terms of the amount of rotational deflection of the vehicle frame, the next step is to describe how much rotational power the engine is creating. Rotational power is defined by the torque and angular velocity of the rotating shaft [Eq. (7)].[8] To calculate the power output of the engine, the angular velocity of the engine $\omega_E(t)$ must be measured. The angular velocity of the engine can be determined directly from the acoustic emissions of the engine. By substituting

Table 1 Predicted engine torque-induced frame twist amounts for an unloaded, half-loaded, and fully loaded semitrailer truck each accelerating at the same constant rate.

	k_s (N/m)	r (m)	θ_0 (deg)	x'' (m/s^2)	m (kg)	Predicted frame twist (deg)
Unloaded	1,300,000	0.8	33	1	18,000	0.75
Half loaded	1,300,000	0.8	33	1	34,000	1.42
Fully loaded	1,300,000	0.8	33	1	51,000	2.15

Eq. (6) into Eq. (7), the power output of the engine can be expressed in terms of the frame twist and the engine frequency (along with several vehicle-specific scalar constants)

$$P_E(t) = \tau_E(t) \cdot \omega_E(t), \tag{7}$$

$$P_E(t) = -\omega_E(t) \cdot k_s \cdot r^2 \cdot \cos[\theta(t) + \theta_0] \cdot \tan\,\theta(t). \tag{8}$$

Assuming that all of the rotational power being generated by the engine is converted into linear vehicle motion, the definite integral of the power output of the engine would be equal to the change in kinetic energy of the vehicle as shown in Eq. (9). Where $\mathrm{KE}(t)$ is the vehicle's kinetic energy at a time t. Substituting the expression for engine power and the standard equation for kinetic energy results in Eq. (10). By assuming that the vehicle is accelerating from a resting state, solving for the mass of the vehicle m, and taking the absolute value of the definite integral Eq. (10) can be expressed in the simplified form shown in Eq. (11). Note that the absolute value of the definite integral is computed because frame twist may be positive or negative depending on the rotation direction of the engine. This equation is appropriate only when the vehicle is accelerating from a stop [in the case of engine idle [$\omega_E(t) > 0$], no frame twist would occur [$\theta(t) = 0$] and the linear velocity would remain zero [$x'(t) = 0$], therefore, the equation that results would be undefined $(m = 0/0)$]

$$\mathrm{KE}(t_f) - \mathrm{KE}(t_0) = \int_{t_0}^{t_f} P_E(t)\mathrm{d}t, \tag{9}$$

$$\frac{1}{2} \cdot m \cdot [x'(t_f)^2 - x'(t_0)^2] = -k_s \cdot r^2 \int_{t_0}^{t_f} \omega_E(t) \cdot \cos[\theta(t) + \theta_0] \cdot \tan\,\theta(t)\mathrm{d}t, \tag{10}$$

$$m = \frac{2 \cdot k_s \cdot r^2 \left| \int_{t_0}^{t_f} \omega_E(t) \cdot \cos[\theta(t) + \theta_0] \cdot \tan\,\theta(t)\mathrm{d}t \right|}{x'(t_f)^2}. \tag{11}$$

From Eq. (11), the mass of the vehicle can be solved for in terms of three dynamic values; the engine's angular velocity $\omega_E(t)$, frame twist angle $\theta(t)$, and the velocity of the vehicle $x'(t)$ along with three vehicle-specific scalar constants; the spring constant of the suspension k_s, the distance from the engine's axis of rotation to the suspension spring r, and the angle of the engine force relative to the suspension spring θ_0. The dynamic values can be measured remotely, however, the scalar constants will need to be estimated based on vehicle type/class.

It should be noted that a method for accurately estimating the scalar constants of a given vehicle has not been identified, and the development of such a method may prove challenging. All of the testing and analysis described here were done independent of the scalar values. The goal of this work was to show definitive correlation among the three dynamic values [the engine's angular velocity $\omega_E(t)$, frame twist $\theta(t)$, and the velocity of the vehicle $x'(t)$] and the vehicle's mass. In order for this methodology to be implemented in any meaningful way, a technique must be devised to accurately measure or estimate the scalar vehicle constants. Furthermore, validation of the relationship among frame twist, engine torque, and the scalar vehicle constants is required.

3 Methodology

In the previous section, a method was described to calculate the mass of a vehicle from three dynamic values and three scalar constants. This section will describe how the three dynamic values can be extracted from remotely sensed video and audio data acquired by a Canon EOS Rebel T2i DSLR camera and free field condenser microphone positioned as shown in Fig. 3.

3.1 *Frame Twist*

The first dynamic value of interest is frame twist, which is a measure of the angular amount that the vehicle's frame is twisting relative to its axles as a function of time. Presented here is a method for measuring the frame twist for a specific truck with a longitudinally mounted engine from video data. This method exploits features unique to this vehicle and would require substantial redevelopment to be appropriate for all vehicles.

Video of the test vehicle was collected from a front-on viewpoint using a conventional Canon EOS Rebel T2i DSLR camera as the vehicle accelerated from a stationary state toward the camera's position. A normalized correlation-based video tracking algorithm was used to track and isolate the same region of the vehicle's grill for each frame (based on the method described by Gonzalez and Woods[9]). The algorithm was designed to track the location of a predefined region, and to be tolerant of small frame-to-frame changes in scale and rotation. An example of the results of the tracking algorithm can be seen in Fig. 4. The grill was chosen for its numerous long parallel lines, which allowed for subpixel measurements of the overall angular orientation to be made. Each isolated grill region extracted by the tracking algorithm was rotated using an affine transformation and bilinear resampling of digital count values. The rotated image was cropped to remove the edge artifacts caused by the

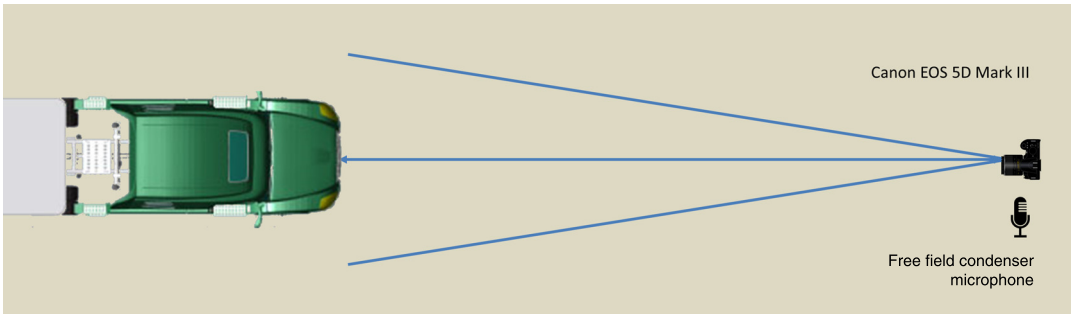

Fig. 3 Diagram of the camera, microphone, and vehicle position during the experiment.

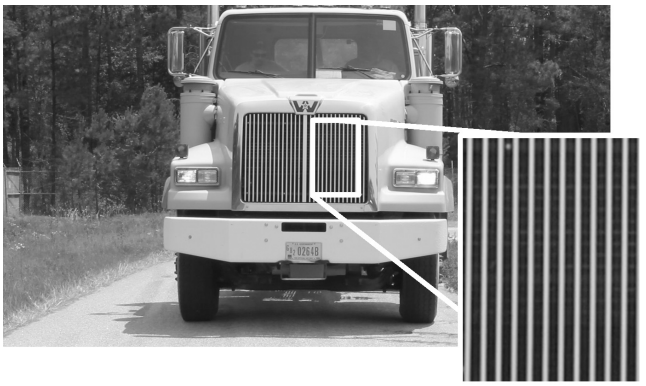

Fig. 4 An image frame with the extracted grill region identified.

rotation, and the summed standard deviation was calculated for each vertical column of pixels in the cropped region using

$$V = \sum_{j=1}^{m} \sqrt{\frac{1}{n} \sum_{i=1}^{n} (x_{i,j} - \bar{x}_j)^2}, \tag{12}$$

where V is a scalar value that quantifies the total vertical variability of the image, m is the number of columns of pixels in the image, n is the number of rows of pixels in the image, $x_{i,j}$ is the intensity value for the pixel at location (i, j), and $\bar{x}_j$ is the average intensity value of the pixels in column j. This scalar value V would have a value of zero if each row of the image was identical. This was repeated for a range of rotation values bounding the expected rotation of the vehicle during its acceleration period. The rotation that resulted in the minimum scalar sum was selected as the rotation of the grill (relative to the vertical image axis). The process was repeated for each image frame as the vehicle was in motion. Figure 5 shows this approach for determining the vehicle's rotation.

3.2 *Position*

The second dynamic value of interest is the position of the vehicle as a function of time. Presented here is a method for measuring the position of a specific vehicle from video data. This method exploits features unique to a specific vehicle and *a priori* knowledge of these features. There are other techniques that could be used to accurately measure a vehicle's position as a function of time that would be more universally applicable, but would require additional equipment (e.g., LiDAR, ultrasonic distance sensor).

Using the same video sequence exploited in the previous section, the camera-to-vehicle distance as a function of time was calculated by observing the spacing of the grill, in pixels, utilizing Fourier analysis. After the grill images were rotated so the grill runs perpendicular to the horizontal image axis, the average of each vertical column was taken, resulting in an averaged grill profile. A Hamming window was applied to the profile to reduce instances of aliasing. The magnitude of the Fourier transform was then taken and the peak frequency was identified as the frequency of the grill, the inverse of this frequency representing the period (in pixels). See Fig. 6 for an example of this process.

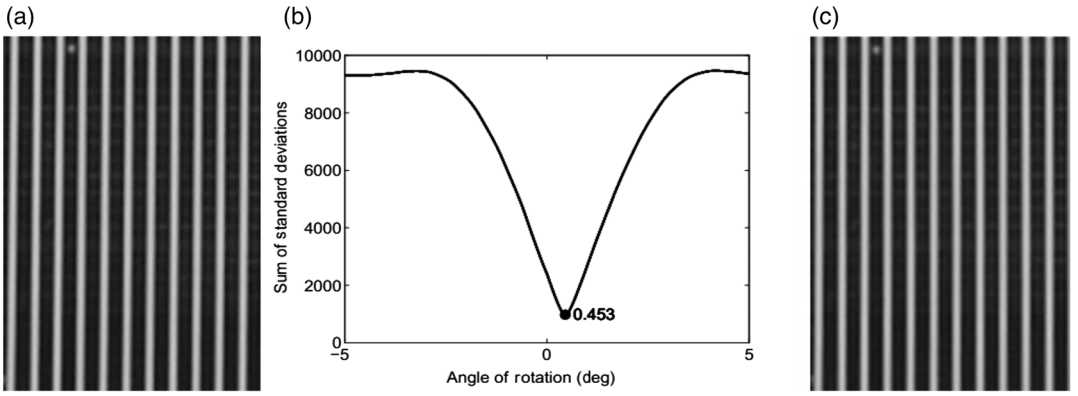

Fig. 5 In order to determine the angle of rotation of the grill, (a) the unrotated grill image is rotated through a range of image rotations from −5 deg to 5 deg, (b) recording the vertical variability as a function of rotation angle. (c) The minimum depicted in the plot corresponds to the position where the grill stands perpendicular to the horizontal image axis.

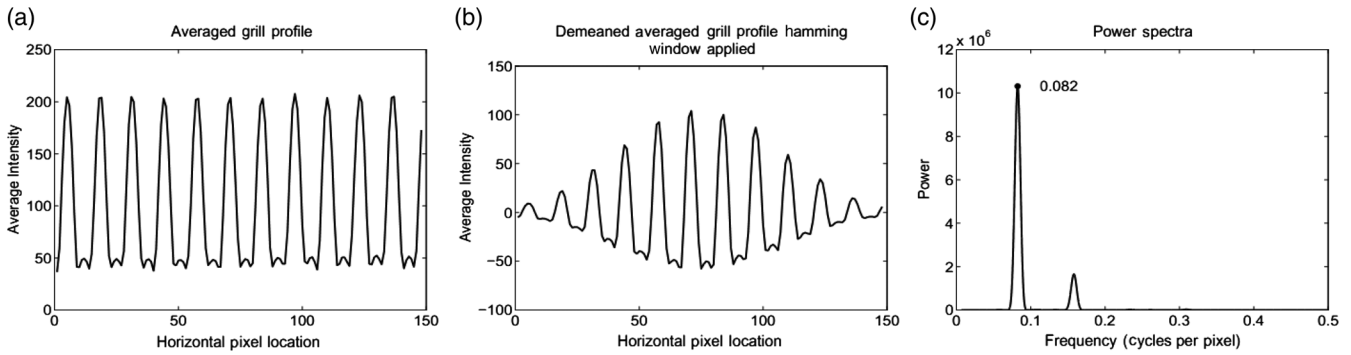

Fig. 6 To calculate the grill spacing, (a) the average grill intensity profile is demeaned and (b) a Hamming window is applied. (c) The power spectra is then calculated and used to find the frequency of the grill.

The grill spacing in pixels was calculated for each video frame using this approach. The camera-to-vehicle distance for each frame was then calculated using Eq. (13), where d is the camera-to-vehicle distance, S is the grill spacing in meters, f is the focal length of the camera in meters, ρ is the pixel pitch of the camera's detector array in meters, and N is the grill spacing in pixels (the period). While the process described here required *a priori* knowledge of the grill spacing, this method could be adapted to work on any feature containing a repetitive, regularly spaced, pattern as long as the camera-to-vehicle distance is known at one point during the collection, or the dimensions of another feature on the vehicle is known (e.g., license plate)

$$d = \frac{S \cdot f}{\rho \cdot N}. \tag{13}$$

3.3 *Engine Speed*

The final dynamic value of interest is engine speed as a function of time. Presented here is a method for measuring the engine speed of a specific vehicle from acoustic data. This method requires *a priori* knowledge of the vehicle's engine size, specifically the number of cylinders. To make this method effective for use on all vehicles, it would need to be modified to determine the number of cylinders from the acoustic data. Preliminary work has been done that suggests that it is possible to calculate the number of cylinders an engine has based on its acoustic signal through analysis of the harmonics.[10]

Acoustic measurements of the test vehicle were collected using a microphone mounted near the path of the vehicle. The audio data were used to calculate the engine speed, again utilizing Fourier analysis. The audio data were first extracted from the video file and converted into a time-based pressure signal. A 0.3-s window of data was selected starting at time zero, a Hamming window was applied, and the magnitude of the Fourier transform was taken resulting in a power spectra. The operating frequency of the engine was calculated by locating the peaks in the power spectra associated with its third, sixth, and ninth harmonic and then dividing the frequency by the harmonic number. For example, if the third harmonic was found at 30 Hz, the engine frequency would be 10 Hz. Three harmonics were used because no single harmonic was found to be reliably persistent in the audio signal. The initial search locations were restricted to frequencies corresponding to the typical idling frequency of a large diesel engine, ~420 to 960 rpm (or 7 to 16 Hz). Once the initial engine frequency was identified, the window of data was moved forward in time by 1 ms and the process was repeated, with the search area for each harmonic being substantially restricted to within 5 Hz of the previous harmonic. If the three harmonics agreed well, the average of the three calculated engine frequency values was used. If one of the three harmonics did not agree, it was discarded. If none of the harmonics agreed well, the lowest order (third harmonic) was selected and used to calculate the engine frequency. This process continued until the entire pressure signal was processed, resulting in an engine frequency versus time signal. An example of this process is shown in Fig. 7.

After the acoustic data were processed into an engine frequency versus time signal, they needed to be synchronized with the data signals extracted from the video (frame twist and camera-to-vehicle distance). This synchronization was achieved through frame-by-frame analysis of on-board video

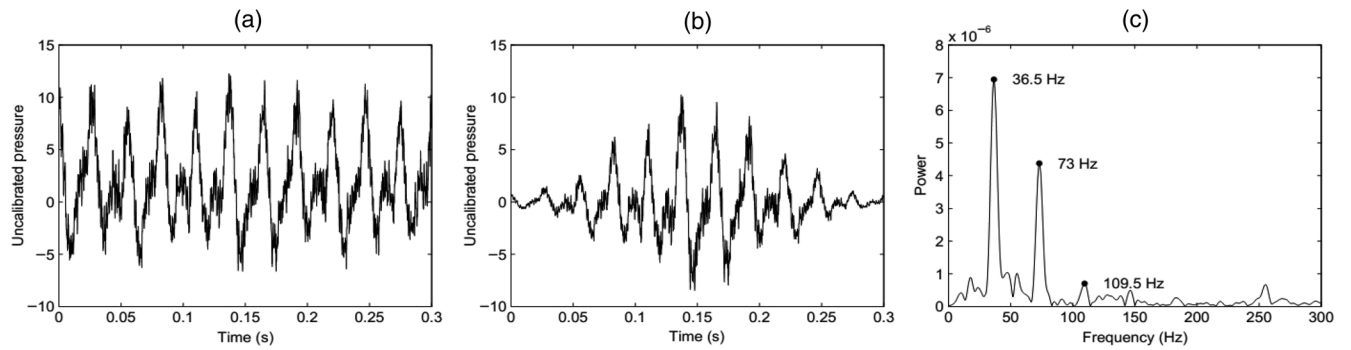

Fig. 7 To calculate engine velocity, (a) the raw acoustic signal is demeaned and (b) a Hamming window is applied. (c) The power spectra is then calculated and used to find the third, sixth, and ninth harmonic.

Fig. 8 An example of the on-board video of the vehicle's instrument panel captured during each test run.

taken from inside the truck during each test run that captured the engine rpm and the vehicle speed from the vehicle's instrument panel. A still frame from this video can be seen in Fig. 8. This method of synchronization was both challenging and imprecise, and it is highly recommended that any future testing utilizes a synchronized data acquisition system to mitigate the need for this approach.

4 Results

Two full-scale field tests were carried out to test the validity of the mass estimation method and the practicality of the remote sensing techniques. Each test was carried out at the Savannah River Site, a United States Department of Energy facility located in Aiken, South Carolina. Both field tests used the same semitrailer truck in three load conditions; the recommended maximum load (40 tons), half the recommended maximum load (20 tons), and no load (empty trailer). Each load mass was determined by loading the trailer with large concrete and metal blocks of known masses. A minimum of three test runs was completed for each load condition during both field tests. The first field test utilized a consumer-quality Canon EOS Rebel T2i DSLR camera positioned in front of the vehicle to collect video and audio as the test vehicle accelerated from a stop. The video was collected at 30 frames-per-second, and the audio was collected at 44.1 kHz. The second field test utilized a Vision Research Phantom v5.1 high-speed video camera in a similar position and collected video at a rate of 1200 frames-per-second. The second test utilized a PCB Piezotronics free-field condenser microphone to collect the audio data at a rate of 52 kHz.

For each test run, the video and audio data were processed using the methods described in the previous section and resulted in angular frame twist, position, and engine speed as a function of time. An example of a processed dataset from the first field test can be seen in Fig. 9 and an example set from the second field test can be seen in Fig. 10. The primary difference between the processed datasets from these two independent field tests was the collection duration. The high-speed camera was able to collect only for a short time (~2 s) due to internal memory limitations and the high frame rate. This resulted in several datasets being deemed unusable because the high-speed video was triggered too late, not capturing the initial frame twist of the vehicle. It is critical that the vehicle is measured while the frame is in a relaxed state; the frame twist at this time correlates to

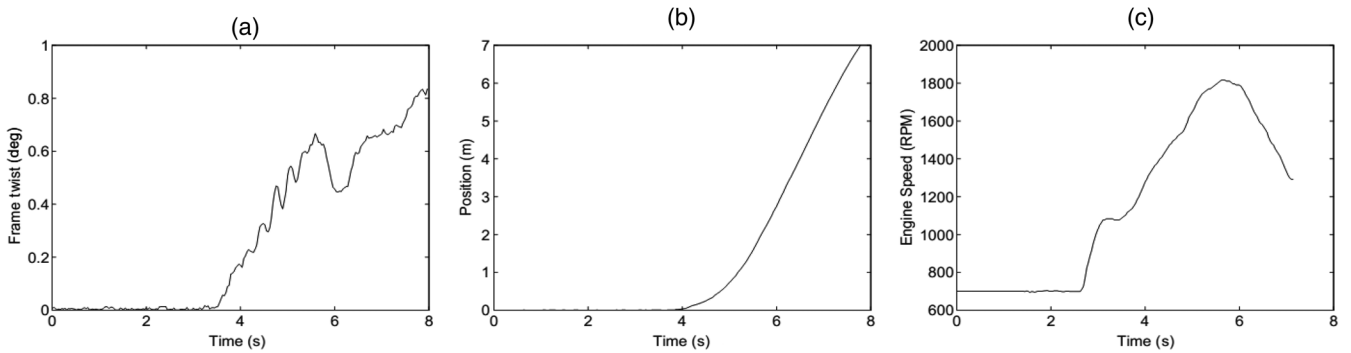

Fig. 9 (a) The angular frame twist, (b) vehicle position, and (c) engine speed of the unloaded test vehicle accelerating from a stop during the first field test.

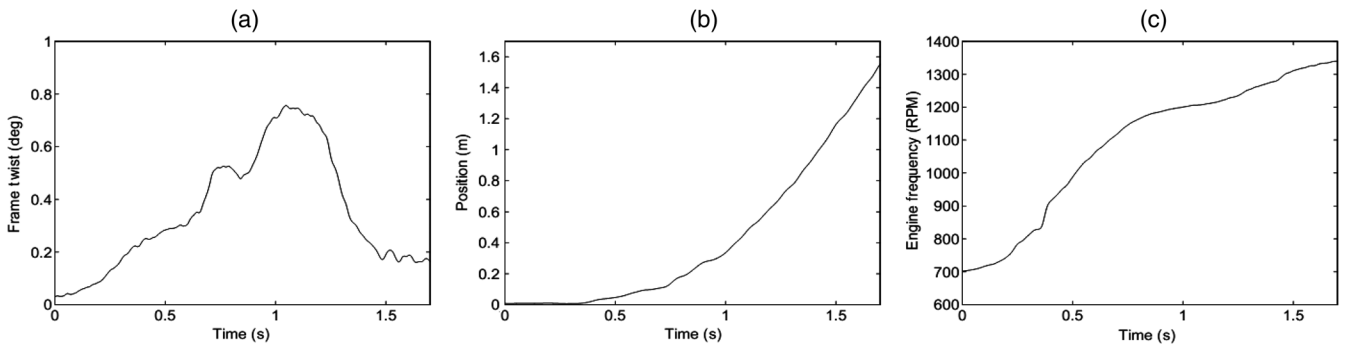

Fig. 10 (a) The angular frame twist, (b) vehicle position, and (c) engine speed of the unloaded test vehicle accelerating from a stop during the second field test.

the zero-torque condition, and all subsequent measurements must be made relative to this initial state. For many of the data sets from the second field test, the high-speed video was initiated after the frame began to twist, but before the vehicle began moving forward (there is typically a 0.5- to 1-s offset between when the frame first twists and the first measurable forward movement of the vehicle occurs). Due to this late initiation of the high-speed video, it was impossible to determine the amount of frame twist associated with the zero torque condition. To mitigate this, the vehicle should be observed for a considerable time, 2 to 3 s prior to acceleration in order to identify the zero-torque frame twist position. It should be noted that the vehicle does not need to be completely stopped in order to identify the zero-torque condition, it must simply not be accelerating at this initial observation.

The spring constant k_s was not known for the test vehicle. As a result, Eq. (11) needed to be modified slightly to account for the unknown spring constant, yielding Eq. (14) which was used to calculate the mass-to-spring constant ratio of the test vehicle for each test run. The final time t_f was identified as the time when the test vehicle reached its peak velocity and the values for r and θ_0 were estimated to be 0.8 m and 33 deg, respectively. The results for the first and second field tests can be seen in Figs. 11 and 12, respectively

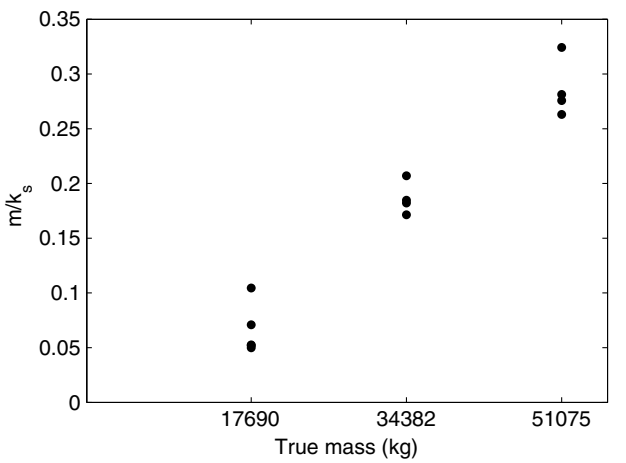

Fig. 11 The calculated mass-to-spring constant ratio for each test run in the first field test versus the true test vehicle mass.

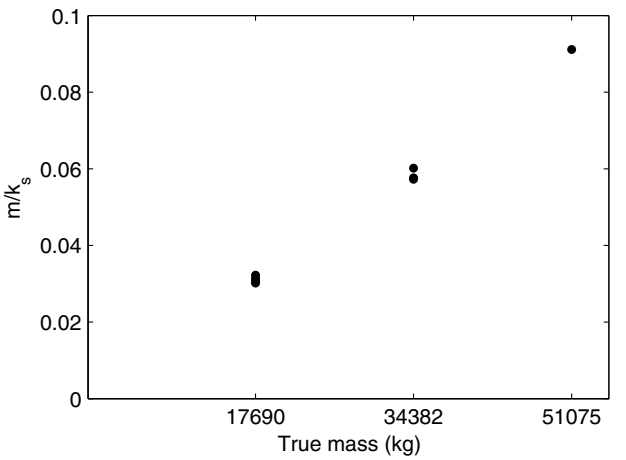

Fig. 12 The calculated mass-to-spring constant ratio for each test run in the second field test versus the true test vehicle mass.

$$\frac{m}{k_s}=\frac{2\cdot r^2\left|\int_{t_0}^{t_f}\omega_E(t)\cdot\cos[\theta(t)+\theta_0]\cdot\tan\,\theta(t)\mathrm{d}t\right|}{x'(t_f)^2}. \tag{14}$$

5 Conclusions

Remotely collected video and audio data were used to calculate a vehicle's position, engine torque-induced frame twist, and engine speed. These signals were used to calculate the vehicle's mass-to-spring constant ratio. The results depicted for the second field test (Fig. 12) show a significant reduction in this mass-to-spring constant ratio when compared to the first field test (Fig. 11). The reduction in this ratio was approximately a factor of three, which suggests that three times as much energy was required, during the first test as compared to the second test, to change the velocity of the test vehicle by the same amount. This discrepancy was investigated and it was determined that the data for the first field test were collected while the test vehicle was driving slightly uphill. Even a mild to moderate incline of 3 deg to 5 deg would account for the discrepancy observed between the two tests. To account for this, future testing would need to be done on roads with an incline of zero degrees, or the incline would need to be incorporated into Eq. (14). The equation for the mass-to-spring constant ratio incorporating the effects of the road surface inclination angle is given here

$$\frac{m}{k_s}=\frac{r^2\left|\int_{t_0}^{t_f}\omega_E(t)\cdot\cos[\theta(t)+\theta_0]\cdot\tan\,\theta(t)\mathrm{d}t\right|}{\left[\frac{1}{2}\cdot x'(t_f)^2\right]+\{-g\cdot[h(t_f)-h(t_0)]\}}, \tag{15}$$

where g is the force due to gravity, $h(t_f)$ is the vehicle's elevation at time t_f, and $h(t_0)$ is the vehicle's elevation at time t_0. This equation shows that a small change in elevation can require a significant amount of energy. For example, an increase in elevation of 5 cm would require the same amount of energy as a change in velocity of 1 m/s.

The correlation between the calculated vehicle mass-to-spring constant ratio and the true vehicle mass was found to be very good for both field tests. The correlation coefficient was calculated to be 97.7% for the first test and 99.7% for the second test. This reflects a very good correlation between the remotely determined values and the true mass data for both experiments. This strong correlation does not reflect accuracy in mass estimation, only that the measured data agreed very well with the actual vehicle mass to within a scale factor. In order for this methodology to calculate vehicle mass, work needs to be done to develop and validate a means of measuring or estimating this scale factor.

The results of this testing showed strong correlation and good within-test repeatability. However, there are multiple areas in which improvements could be made. First, it is critical that all of the measured signals are synchronized. The most accurate method of achieving this synchronization is by utilizing a single data acquisition system for all measurements (audio and video). Second, the data acquisition system must begin measuring the vehicle at least 2 s prior to any forward motion or acceleration from a constant velocity initial motion state. This will ensure that the zero-torque condition is captured. Third, the grade of the road where the test vehicle is being operated should be measured precisely and accounted for using Eq. (15). Finally, observation of the test vehicle should be extended. Increasing the measurement

window to 10 to 15 s should improve the overall effectiveness of the system and make the measurements more robust to noise and measurement error. This could be achieved by reducing the frame rate of the video acquisition system, as the 1200 frames-per-second rate of the Vision Research Phantom v5.1 camera proved to be faster than is required. A more reasonable 100 to 300 frame rate camera should provide more than adequate temporal resolution.

Acknowledgments

The authors would like to thank the United States Department of Energy, National Nuclear Security Administration, and Office of Defense Nuclear Nonproliferation (NA-22) for their support of this work under Contract No. DE-AC09-08SR22470/AC799980. Special thanks are expressed to Dr. Alfred Garrett, Dr. David Coleman, and Dr. Larry Koffman of the Savannah River National Laboratory for their invaluable assistance in facilitating the field experiments carried out at the Savannah River Site in Aiken, South Carolina.

References

1. M. Ghosn et al., "Effects of overweight vehicles on NYSDOT infrastructure," Tech. Rep. (2015).
2. B. Jacob and V. Feypell-de La Beaumelle, "Improving truck safety: potential of weigh-in-motion technology," *IATSS Res.* **34**(1), 9–15 (2010).
3. K. Dey et al., "Estimation of pavement and bridge damage costs caused by overweight trucks," *Transp. Res. Rec. J. Transp. Res. Board* **2411**, 62–71 (2014).
4. D. Podborochynski et al., "Quantifying incremental pavement damage caused by overweight trucks," in *Conf. on Exhibition of the Transportation Association of Canada* (2011).
5. K. Helmi, T. Taylor, and F. Ansari, "Shear force–based method and application for real-time monitoring of moving vehicle weights on bridges," *J. Intell. Mater. Syst. Struct.* **26**(5), 505–516 (2015).
6. A. Irimescu, L. Mihon, and G. Pădure, "Automotive transmission efficiency measurement using a chassis dynamometer," *Int. J. Automot. Technol.* **12**(4), 555–559 (2011).
7. F. Beer, E. Johnston, and J. DeWolf, *Mechanics of Materials*, McGraw-Hill, New York (2002).
8. J. Walker et al., *Fundamentals of Physics*, Wiley, New York (2008).
9. R. Gonzalez and R. Woods, *Digital Image Processing*, Pearson/Prentice Hall, Upper Saddle River, New Jersey (2008).
10. T. McKay, *Detection of Anomalous Vehicle Loading*, PhD Thesis, Rochester Institute of Technology (2016).

Troy R. McKay received his BA degree in applied physics from SUNY Geneseo in 2003, his MS degree in electrical engineering from SUNY Buffalo in 2007, and his PhD in imaging science from the Rochester Institute of Technology in 2016. He is currently the founder and president of Hyperspectral Solutions, LLC.

Carl Salvaggio received his BS and MS degrees in imaging science from the Rochester Institute of Technology (RIT) in 1987, and his PhD in environmental resource engineering in 1994 from the State University of New York College of Environmental Science and Forestry at Syracuse University. From 1994 to 2002, he worked on model validation and database development for the defense intelligence community. Since 2002, he has been a professor of imaging science at RIT.

Jason W. Faulring received his BS degree in computer engineering from the Rochester Institute of Technology (RIT) in 2003. As a senior systems engineer at the Remote Sensing Laboratory of RIT from 2003 to 2015, he developed innovative airborne and ground-based sensing systems for the lab's research efforts. He is currently a senior engineer and partner at AppliedLogix, LLC developing custom hardware and software solutions.

Glenn D. Sweeney received his BS degree in imaging science from the Rochester Institute of Technology in 2013, and his MSc degree in color science from the CIMET University consortium in 2015. After graduation, he has entered the workforce designing image quality test equipment for mobile camera systems.